Advanced Composite Materials
Publication details, including instructions for authors and subscription information:
http://www.tandfonline.com/loi/tacm20

Dispersion and Related Properties of Acid-Treated Carbon Nanotube/Epoxy Composites using Electro-Micromechanical, Surface Wetting and Single Carbon Fiber Sensor Tests

Joung-Man Park [a] , Jung-Hoon Jang [b] , Zuo-Jia Wang [c] , Dong-Jun Kwon [d] , Ga-Young Gu [e] , Woo-Il Lee [f] , Jong-Kyoo Park [g] & K. Lawrence Devries [h]

[a] School of Materials Science and Engineering, Engineering Research Institute, Gyeongsang National University, Jinju 660-701, Korea, Department of Mechanical Engineering, The University of Utah, Salt Lake City, Utah 84112, USA;, Email: jmpark@gnu.ac.kr

[b] School of Materials Science and Engineering, Engineering Research Institute, Gyeongsang National University, Jinju 660-701, Korea

[c] School of Materials Science and Engineering, Engineering Research Institute, Gyeongsang National University, Jinju 660-701, Korea

[d] School of Materials Science and Engineering, Engineering Research Institute, Gyeongsang National University, Jinju 660-701, Korea

[e] School of Materials Science and Engineering, Engineering Research Institute, Gyeongsang National University, Jinju 660-701, Korea

[f] School of Mechanical and Aerospace Engineering, Seoul National University, Seoul 151-742, Korea

[g] Agency for Defense Development, 4-R and D Center, Daejeon 305-600, Korea

[h] Department of Mechanical Engineering, The University of Utah, Salt Lake City, Utah 84112, USA

Version of record first published: 02 Apr 2012.

VSP

Advanced Composite Materials 20 (2011) 337–360

ADVANCED COMPOSITE MATERIALS
brill.nl/acm

Dispersion and Related Properties of Acid-Treated Carbon Nanotube/Epoxy Composites using Electro-Micromechanical, Surface Wetting and Single Carbon Fiber Sensor Tests

Joung-Man Park [a,d,*], **Jung-Hoon Jang** [a], **Zuo-Jia Wang** [a], **Dong-Jun Kwon** [a], **Ga-Young Gu** [a], **Woo-Il Lee** [b], **Jong-Kyoo Park** [c] **and K. Lawrence DeVries** [d]

[a] School of Materials Science and Engineering, Engineering Research Institute, Gyeongsang National University, Jinju 660-701, Korea

[b] School of Mechanical and Aerospace Engineering, Seoul National University, Seoul 151-742, Korea

[c] Agency for Defense Development, 4-R and D Center, Daejeon 305-600, Korea

[d] Department of Mechanical Engineering, The University of Utah, Salt Lake City, Utah 84112, USA

Received 12 July 2010; accepted 19 November 2010

Abstract

Studies of dispersion and related properties, in carbon nanotube/epoxy composites, were conducted using electro-micromechanical and wettability tests. Specimens were prepared from neat epoxy as well as composites with untreated and acid-treated carbon nanotube (CNT). The degree of dispersion and its standard deviation were evaluated by turbidity of the dispersing solution, as well as by volumetric electrical resistivity. Acetone was a better dispersing solvent than purified water and various acid treatments of the CNT also enhanced dispersion. Contact resistivity responded differently with dispersion degree. The apparent Young's modulus was higher for composites with acid treated CNT. The interfacial shear strength between a single carbon fiber and CNT/epoxy was lower than that between a single carbon fiber and neat epoxy. This difference is attributed to increased viscosity and decreased bonding availability in the matrix due to the added CNT. The optimum CNT treatment, for maximizing interfacial adhesion while maintaining good electrical conductivity was the sulfuric acid treatment. The CNT composites can also sense micro-damage in terms of the stepwise increments of electrical resistivity combined with acoustic emission.

Keywords

Carbon nanotube, dispersion, interfacial shear strength, electrical resistance, electro-micromechanical test

* To whom correspondence should be addressed. E-mail: jmpark@gnu.ac.kr
Edited by the KSCM

DOI:10.1163/092430410X550881

1. Introduction

The unique properties of carbon nanotubes (CNT) have led to their use as reinforcing fillers for composites. The CNT/based composites have been studied intensively with various polymer matrices and show great promise for use in applications in aerospace, transportation and other industries [1–3]. The considerable attention they have recently received is in large part due to their unique mechanical, surface and multi-functional properties. They exhibit a strong interaction with the matrix which is associated with their nano-scale microstructure and extremely large specific interfacial area [4]. CNT is typically subjected to a variety of different chemical treatments to create chemical functionality thereby improving dispersion, interfacial adhesion, and/or matrix compatibility that results in enhanced processability and properties. It has been demonstrated, for example, that chemical modification of CNT can significantly enhance its dispersion in various solvents [5–7]. For lack of a better name, the dispersion agent is called a solvent throughout this paper, although it is recognized that CNT is a suspension rather than a solute in the dispersing liquids.

Carbon nanomaterials (CNM) have high specific surface areas and can easily aggregate. Surface functionalization of CNM is an effective method for enhancing dispersion in various media thereby producing new functional materials, with unique characteristics and properties [8, 9]. In order to functionalize CNM, the surface needs to be treated with acids or other chemicals. Treatment of the CNM with either nitric acid or sulfuric acid leads to surface oxidation forming oxidized groups such as carboxyl and carbonyl groups within the graphene sheet [10–13]. The surface functional groups of modified CNM are often characterized by FT-IR or Raman spectroscopy. It is difficult, however, to obtain quantitative information of the chemical species existing in a monolayer or only a few layers of the oxidized surface of CNM by these analyses.

Currently, in an effort to increase strength and toughness, researchers are planning to use CNT in polymer composites for practical applications, especially as an additional filler in the fiber–matrix macroscopic polymer composites. During fiber breakage or interfacial debonding, in these macroscopic polymer composites, CNT at the interface might bridge cracks. This could improve the interfacial shear strength (IFSS) and toughness in these macroscopic composites [14].

Electro-micromechanical techniques have been developed and used as efficient nondestructive evaluation (NDE) methods for sensing micro-damage in the characterization of interfacial properties. In this technique, a single partially embedded conductive fiber acts as both a sensing element and a reinforcing fiber [15, 16]. In the study reported here, the single carbon fiber sensing and the reinforcing effects for three types of acid-treated CNT/epoxy composites were investigated, using measurements of electrical resistance and wettability. These electrical properties and interfacial evaluations in carbon composites were then correlated with the different types of acid treatments of the CNT.

2. Experimental

2.1. Materials

Multi-wall carbon nanotubes (CNT, Iljin Nanotech Co., Korea) with diameters of 10–25 nm, aspect ratios of 400–1000 and a density of 1.55 g/cm^3 were used for composite reinforcement. Carbon fibers (T700S, Toray Inc., Japan), with an average diameter of approximately 8 μm were used as the single fiber sensor. Epoxy resin (YD-114, Kukdo Chemical Co., Korea) based on dilute diglycidyl ether of bisphenol-A was used as an inner matrix, with KBH-1089 (Kukdo Chemical Co., Korea) based on acid anhydride, as the hardener. The outer matrix epoxy resin (TD-127, Kukdo Chemical Co., Korea) was used with polyoxypropylene diamine (Jeffamine D-400 and D-2000, Huntsman Petrochemical Co.) as ductile curing agent and KH-100 (Kukdo Chemical Co., Korea) as a rigid curing agent. Two solvents were used for dispersion of the CNT, i.e., acetone, and two times purified water. Three acids, i.e., H_2SO_4, HNO_3 and $Na_2Cr_2O_7$, were used for cleaning and treating the CNT. The four probe liquids used for contact angle measurements were two times purified water, formamide, diiodomethane, and ethylene glycol.

2.2. Methodologies

2.2.1. Acid Treatment on CNT and Dispersion Process in Epoxy

Figure 1 shows schematically the processes used for: (a) acid treatment and (b) dispersion of the CNT for use in the CNT/epoxy composites. The CNT was treated using three different acids, i.e., HNO_3, H_2SO_4 and $Na_2Cr_2O_7 + H_2SO_4$. The acid, at a concentration of 30 wt% in water, was used to treat the CNT for 10 min at 50°C in an oven. After the acid treatment the CNT was thoroughly washed, using distilled water, and then dried for 3 days at 60°C in a vacuum oven. As outlined in Fig. 1(b), after acid treatment, the CNT was added to the dispersion solvent (either acetone or water) and dispersed by sonication for 2 h. The epoxy resin was next poured into the CNT solution and mechanically mixed, followed by sonication on the mixture for 18 h, in an enclosed beaker. This solution was then further treated, by sonication, in an open beaker for 2 h at room temperature, to facilitate evaporation of the solvent. Then the dispersive solvent was further removed from the solution by evaporation under sonication at 35°C for 3 days. Any residual solvent was eliminated in a vacuum oven at 50°C, for 3 days. The final steps in the preparation of the CNT/epoxy specimen involved the addition of the curing agent, pouring this mixture into a mold and allowing it to cure as described later.

2.2.2. Electrical Resistivity Measurement

Figure 2 shows the layout of the specimen used for measurement of electrical volumetric resistivity by the four-point method. Note the adjective volumetric is used here to make clear that this resistivity is the resistance per unit volume in contrast to the contact resistivity defined as the resistance per unit area as discussed in the next section. Electrical contact points were located at regular intervals using cop-

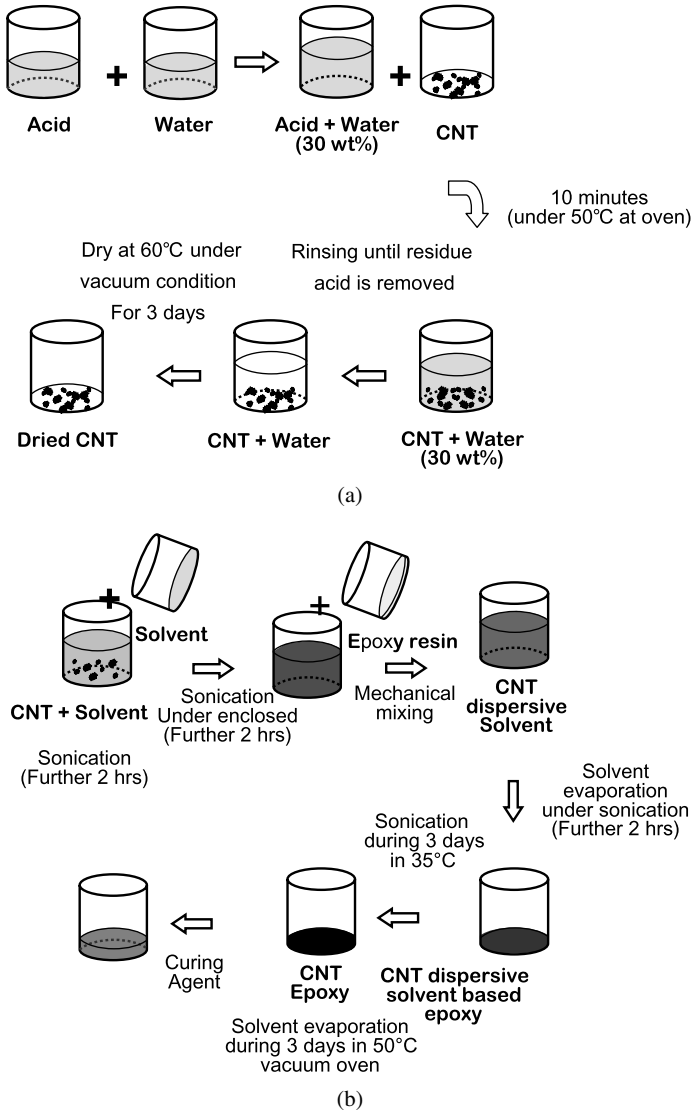

Figure 1. Schematic of the processes used for acid treatment and dispersion of the CNT: (a) acid treatment and (b) dispersion.

per wire and silver paste. The volumetric electrical resistivity, ρ_v, was calculated from the measured electrical volumetric resistance, R_v, the cross-sectional area of the CNT/epoxy composites, A_v, and electrical contact length, L_{ec} of the testing specimen by the following relationship:

$$\rho_v = \left(\frac{A_v}{L_{ec}}\right) \times R_v \ (\Omega \cdot \mathrm{cm}). \tag{1}$$

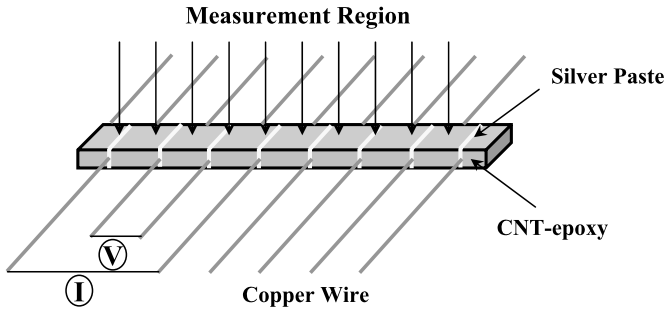

Figure 2. Schematic of the layout of the experimental specimen for measuring volumetric electrical resistivity using the four-point method.

2.2.3. Measurement of Apparent Young's Modulus and the Electrical Contact Resistivity

A single carbon fiber sensor in a carbon fiber/CNT/epoxy composite under cyclic strain was used as test specimens in an electro-pull test. Figure 3 shows schematically the experimental specimens used for measuring: (a) apparent Young's modulus and (b) electrical contact resistivity. In this study, the apparent Young's modulus is defined as the stress in the bare fiber (load/fiber area) divided by the effective strain of the carbon fiber (change in length of both the embedded and bare segments/initial length) in the specimen shown in Fig. 3(a). Clearly, if the CNT/epoxy composite had no reinforcing effect on the fiber (i.e., no interfacial bonding) the apparent Young's modulus would be simply the Young's modulus of the bare carbon fiber. Therefore, the difference of the apparent Young's modulus from this base value provides a convenient indirect measure of the IFSS or stress transfer between the carbon fiber and the CNT/epoxy composite.

In both the apparent Young's modulus and the contact resistivity experiments, the specimens were exposed to constant amplitude cyclic strain using a mini-Universal Testing Machine (UTM) (H1KS, Hounsfield Equipment Ltd., UK), with an attached multimeter (HP34401A, USA). A 100 N load cell was used and the specimens were exposed to cyclic triangular waveform deformation with a loading/unloading rate of 0.5 mm/min. The specimens were loaded into the mini-UTM grips, and the multimeter was connected electrically to the carbon fiber with thin copper wires as shown in Fig. 3(a). The reinforcing effect was determined indirectly by the apparent Young's modulus test under cyclic loading as described in the previous paragraph.

During the electro-pull test, the change in electrical resistance, ΔR, was measured during the cyclic fiber tension, along the path involving the conductive matrix, the interface and the segment of the carbon fiber between the voltage measuring points shown in Fig. 3(b). The total electrical resistance, R_T, is related to the volumetric resistances of the fiber, R_v^{fiber} and composite, $R_v^{composite}$, and the contact resistance, R_c, between the fiber and the sample matrix by:

$$R_T = R_v^{fiber} + R_c + R_v^{composite}. \tag{2}$$

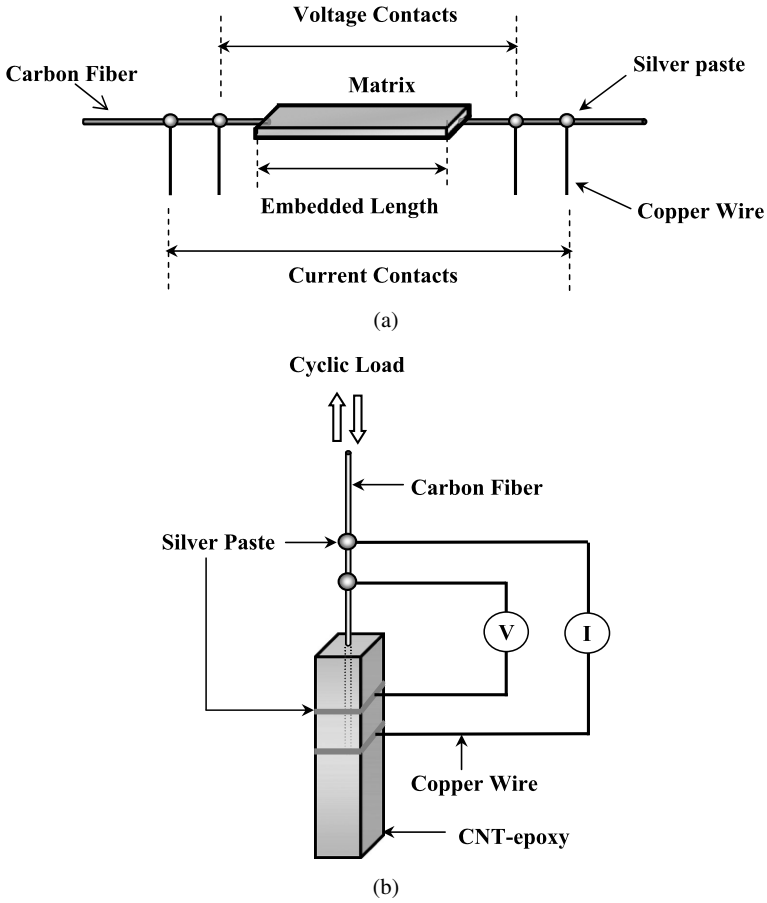

Figure 3. Experimental specimens for measurement of (a) apparent Young's modulus and (b) contact resistivity during constant amplitude cyclic strain tests.

The experiments indicated, however, that this total electrical resistance, R_T, was largely dominated by the contact resistance at the carbon–composite interface, R_c. For making these measurement by the four-point method two electrical contacts were formed on the carbon fiber and the other two electrical contacts were formed around the perimeter of the CNT/epoxy composite.

2.2.4. Preparation of Microdroplet Specimens and IFSS Measurement

The IFSS between the carbon fiber and the CNT/epoxy surface was measured by a microdroplet test which can be described as follows. Carbon fibers were fixed at regularly spaced intervals in a steel frame. Microdroplets of CNT/epoxy composite were formed on each carbon fiber using a pin tip (as described in Section 3.3 and shown in the photographs of Fig. 12), followed by curing for 2 h in an oven at 120°C. For testing of these samples, one end of the fiber was attached by epoxy adhesive to a paper strip. This paper strip was fixed in a clip–grip attached to load cell

in a UTM (LR 10K, Lloyd Co., UK). The microdroplet, on the specimen, was held in place for pullout testing by a specially designed microvice composed of two thin plates brought into near contact with the carbon fiber, just above the microdroplet. The IFSS, τ was calculated from the measured pullout force, F using the following equation:

$$\tau = \frac{F}{\pi D_f L}, \tag{3}$$

where D_f and L are the fiber diameter and the length of fiber embedded in the matrix.

2.2.5. Measurement of Wettability and Surface Energies

Dynamic contact angle [17, 18] was determined by the Wilhelmy plate method (Sigma 70, KSV Co., Finland) for evaluating wettability and surface energy, rather than by conventional static contact angle measurements. The 'plates' used in these tests were either single carbon fibers or small plates of CNT/epoxy composites. The dynamic contact angles of carbon microfiber for each of different acid-treated CNT/epoxy composites, and for neat epoxy were determined from the plate immersion pullout values using standard methods and techniques for the Wilhelmy plate method [17, 18]. Four dipping liquids were used for these tests, i.e., two times purified water, formamide, ethylene glycol and diiodomethane. Donor and acceptor components, and polar and dispersive free energy terms were calculated from the dynamic contact angle values. The basic equation for the Wilhelmy plate method is:

$$F = mg + P\gamma_{LV}\cos\theta - F_b, \tag{4}$$

where F is total force, m is the mass of the plate, g is the acceleration of gravity, F_b is the buoyancy force, P is the fiber perimeter, γ_{LV} is the surface tension of the liquid, and the difference $F - mg$ is equal to the measured force. Because the value of the buoyancy force is zero at the immersing interface, equation (4) can be rearranged as:

$$\cos\theta = \frac{Mg}{\pi D\gamma_{LV}}, \tag{5}$$

where Mg is the experimentally measured force.

The total surface energy, γ^T is the sum of the Lifshitz–van der Waals component, γ^{LW} and the acid–base component, γ^{AB} which for a solid and a liquid this can be expressed as:

$$\gamma_S^T = \gamma_S^{LW} + \gamma_S^{AB}, \qquad \gamma_L^T = \gamma_L^{LW} + \gamma_L^{AB}. \tag{6}$$

The acid–base component (or hydrogen bonding) includes the electron acceptor, γ^+ and the electron donor, γ^- components, which are not additive and can be expressed for a solid and a liquid as:

$$\gamma_S^{AB} = 2\left(\gamma_S^+\gamma_S^-\right)^{1/2}, \qquad \gamma_L^{AB} = 2\left(\gamma_L^+\gamma_L^-\right)^{1/2}. \tag{7}$$

With the modified Young–Dupre equation the above components can be used to obtain the work of adhesion, W_a, as:

$$W_a = \gamma_L(1+\cos\theta) = 2\left(\gamma_L^{LW}\gamma_S^{LW}\right)^{1/2} + 2\left[\left(\gamma_S^-\gamma_L^+\right)^{1/2} + \left(\gamma_S^+\gamma_L^-\right)^{1/2}\right]. \quad (8)$$

The value of γ_S^{LW} for the solid is evaluated from the contact angle for a polar liquid, which is a non-polar liquid without donor and acceptor components, such as diodomethane on the solid and equation (8) reduces to:

$$\gamma_L(1+\cos\theta) = 2\left(\gamma_L^{LW}\gamma_S^{LW}\right)^{1/2}. \quad (9)$$

This equation assumes that the liquid has negligible acid–base interaction with the solid. It is also assumed that γ_L, γ_L^{LW} and γ_L^+ and γ_L are known for the testing liquids and that $\cos\theta$ can be determined using equation (5). With known values of γ_S^{LW} and the contact angles obtained using different liquids on the solid, the two resulting equations (8) can be solved simultaneously to obtain the values of γ_S^+ and γ_S^+ for the two test solvent sets.

A commonly-used approach in considering solid surface energies is to express them as a sum of dispersive and polar components which can influence the work of adhesion, W_a between the surface of the reinforcement material and the matrix. To determine the polar and dispersive surface free energies, the Owens–Wendt equation [19] is used, expressed as:

$$W_a = \gamma_L(1+\cos\theta) = 2\left(\gamma_S^d\gamma_L^d\right)^{1/2} + 2\left(\gamma_S^p\gamma_L^p\right)^{1/2}, \quad (10)$$

where γ_L, γ_{Ld} and γ_L^p are known for the testing liquids and γ_S^p and γ_S^d can be calculated from the measured contact angles. In this way, the dispersive and acid–base components of both the reinforcement material and the matrix can be determined. It is possible to calculate the work of adhesion, W_a between the embedded the carbon fiber (F) and the CNT/epoxy matrix (M) at the interface, using the equation:

$$W_a = 2\left[\left(\gamma_F^{LW}\gamma_M^{LW}\right)^{1/2} + \left(\gamma_F^-\gamma_M^+\right)^{1/2} + \left(\gamma_F^+\gamma_M^-\right)^{1/2}\right]. \quad (11)$$

2.2.6. Acoustic Emission Measurements using a Double-Matrix Composite Specimen

Figure 4 shows the experimental layout for micro-damage sensing, using electrical resistance and acoustic emission (AE) (Mistras 2001 System, Physical Acoustics Co., USA). The double-matrix composites (DMC) specimens, used for this study, were composed of a single carbon fiber embedded in a brittle layer of CNT/epoxy surrounded by an outer more ductile epoxy support layer. The DMC test was designed to provide information and insight into the IFSS of the interface between the carbon fiber and the inner more brittle layer. During testing, the DMC test was performed to monitor carbon fiber fracture and/or slippage of the carbon fiber embedded in the inner conductive composite.

To prepare a sample for the DMC test, the carbon fiber was situated and fixed in a silicone mold. The CNT/epoxy mixture was then poured into the mold, and

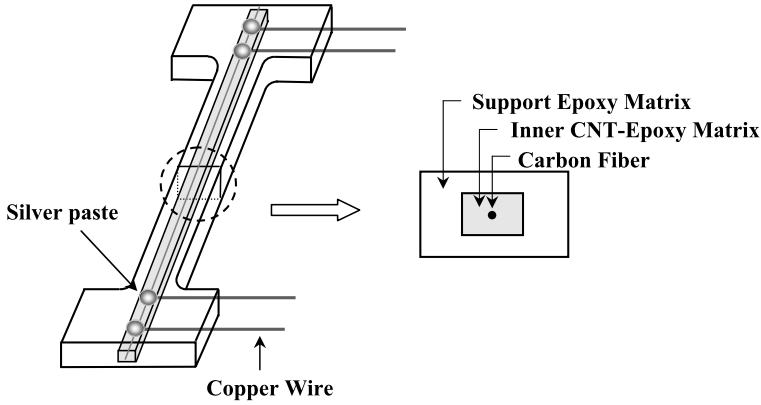

Figure 4. Schematic of the experimental system used for micro-damage sensing by means of electrical resistance and AE measurements.

pre-cured at 80°C for 2 h. The final step in the sample preparation was to situate this single carbon fiber/CNT/epoxy inner strip into the dog-bone silicone mold and filling it with the ductile epoxy and curing at 80°C for 2 h, followed by a post-cure for 2 h at 120°C. The DMC specimens used for determination of AE parameters and electrical resistance were tested in tension using another mini-UTM (Pico Industrial Inc., Korea) with a 100 kg_f load cell at a test speed of 0.5 mm/min. The change in electrical resistivity, associated with fiber fracture, was measured and correlated with the simultaneously measured AE parameters. Such AE measurements, in combination with micromechanical tests, have been used to provide information and insight into the fundamental microfailure mechanisms occurring in composite materials [20]. The test specimen was loaded into the grips of the UTM and an AE-Piezoelectric Transducer (PZT) was attached to the center of the sample, using vacuum grease. The AE-PZT output was amplified by a 40 dB preamplifier and passed through a 100 to 1000 kHz band-pass filter, at a threshold level of 40 dB. The elastic waves resulting from microfailure were transformed to voltage signals by the PZT sensor, amplified and recorded as AE parameters.

3. Results and Discussion

3.1. Comparison of Dispersion of CNT for the Two Dispersion Solvents

Figures 5 and 6 show the turbidity of CNT with different acid treatments at different elapsed times in acetone and two times purified water. These two solvents were chosen as 'good candidates' from recent prior work [21]. These measurements of the degree of dispersion, as evidenced by the turbidity for different elapsed times, were preformed after 2 h of sonication and with a CNT concentration of 0.02% by weight. Different turbidity was exhibited as a result of the difference in degree of dispersion and stability in acetone (Fig. 5) and water (Fig. 6). The degree of dispersion could be also varied through the use of different acid treatments. The

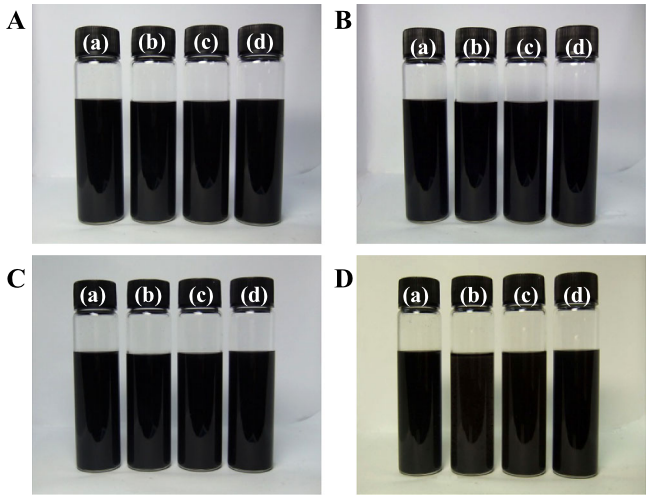

Figure 5. Comparison of turbidity of 0.02 wt% CNT in acetone for different CNT treatments: (A) untreated; (B) H_2SO_4; (C) HNO_3 and (D) $Na_2Cr_2O_7 + H_2SO_4$ after different elapsed times: (a) initial; (b) 30 min; (c) 3 h and (d) 12 h. This figure is published in color in the online version.

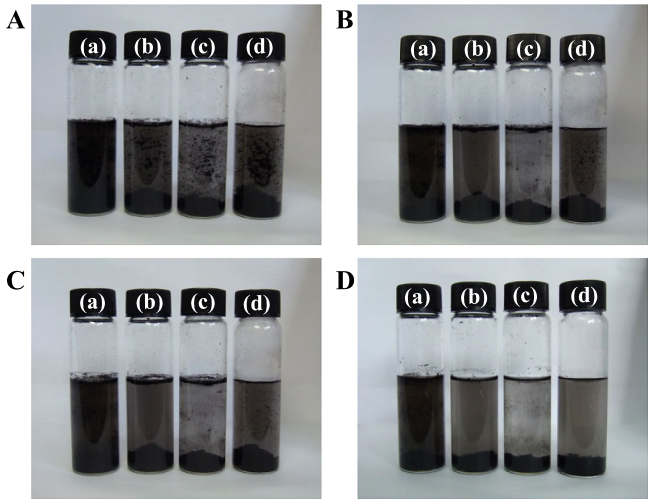

Figure 6. Comparison of turbidity of 0.02 wt% CNT in water for different CNT treatments: (A) untreated; (B) H_2SO_4; (C) HNO_3 and (D) $Na_2Cr_2O_7 + H_2SO_4$ after different elapsed times: (a) initial; (b) 30 min; (c) 3 h and (d) 12 h. This figure is published in color in the online version.

turbidity in acetone was much more stable than that in water. Untreated CNT was also more stable, in the acetone solvent, than was acid-treated CNT.

Figure 7 shows field emission scanning electron microscope (FE-SEM) photographs of the fracture surfaces for 0.5 vol% CNT/epoxy composites. These samples were prepared using acetone as the dispersion solvent and with the four

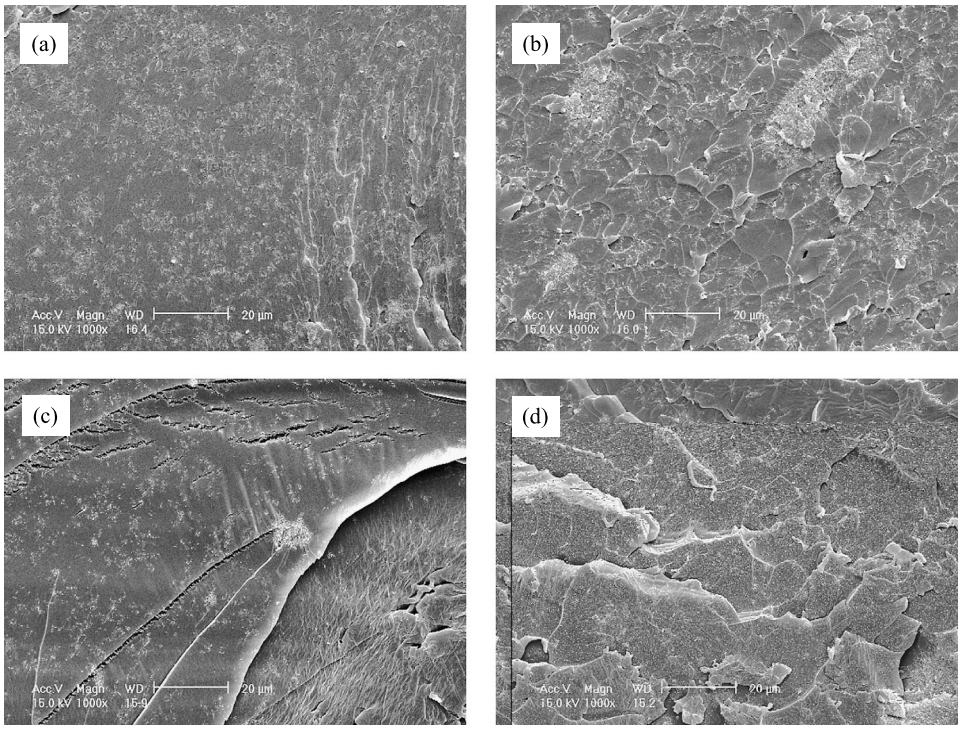

Figure 7. FE-SEM photographs of fracture surfaces for 0.5% CNT–epoxy nanocomposites with different CNT treatments with acetone solvent: (a) untreated; (b) H_2SO_4; (c) HNO_3 and (d) $Na_2Cr_2O_7 + H_2SO_4$.

different CNT treatments: (a) untreated; (b) H_2SO_4; (c) HNO_3 and (d) $Na_2Cr_2O_7 + H_2SO_4$. The fracture surface morphology of CNT/epoxy composites was observed to depend on the comparative degree of dispersion of the CNT. The degree of dispersion was likewise found to depend on the dispersion solvent and the acid treatments. As a general rule, better dispersion resulted in composites with smoother fracture surfaces.

Figure 8 shows the volumetric electrical resistivity of CNT for the two solvents. The degree of dispersion of the CNT/epoxy composite was affected by both the type of dispersion solvent and the type of acid treatment used. Better dispersion generally resulted in lower electrical resistivity, which is attributed to better distribution of the CNT in the matrix as well as more and better electrical contact. Consequently, the degree of dispersion in CNT/epoxy composite using acetone for dispersion was better than that using water. The volumetric electrical resistivity of acid-treated CNT was generally somewhat higher than it was for untreated CNT in epoxy matrices. This is attributed to the fact that acid-treated CNT composites are less conductive due mainly to polymeric functionalization on the CNT surfaces, even though they typically exhibit improved interfacial adhesion. The

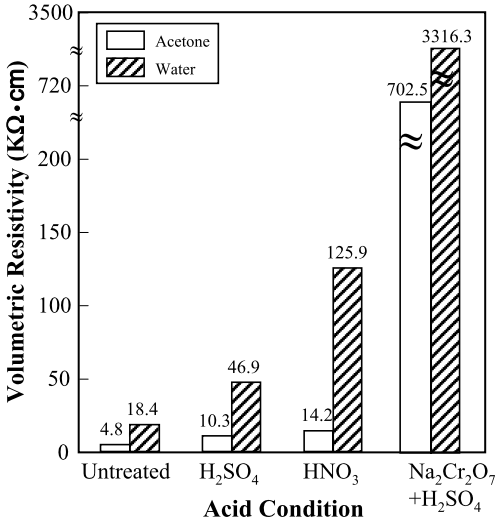

Figure 8. Volumetric resistivity of CNT/epoxy composites for different CNT treatments with acetone and water dispersion solvents.

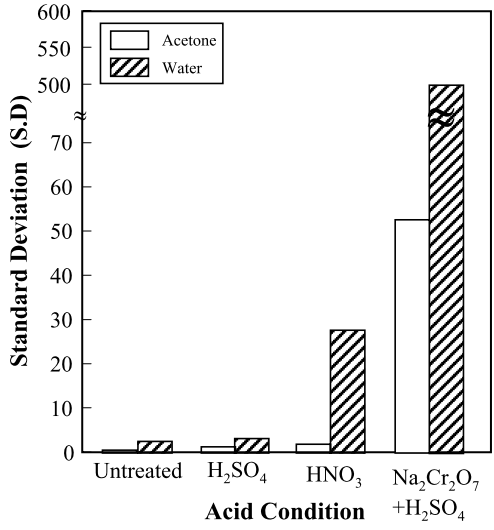

Figure 9. Comparison of the SD of the volumetric resistivity for composites of untreated and the three acids-treated CNT/epoxy composites.

$Na_2Cr_2O_7 + H_2SO_4$ treated material exhibited poor dispersion and the resulting composites had extremely high volumetric resistivity, comparatively speaking.

Figure 9 shows a comparison of the standard deviation (SD) of volumetric electrical resistivity of CNT in epoxy for different CNT treatments. The SD value can be closely correlated with the comparative degree of dispersion which was also related to the probability of the degree of electrical contact between the CNTs. The

SD for composites with acid-treated CNT was somewhat larger than the SD for the composites with untreated CNT, which the authors had not expected. Although the acid treatments did not significantly affect electrical conductivity, the associated enhanced interfacial adhesion generally resulted in improvement in mechanical properties.

3.2. Load Sensing of a Single Carbon Fiber Embedded in Acid-Treated CNT/Epoxy Composites

Figure 10 shows (a) a plot of apparent stress *versus* strain and (b) the apparent Young's modulus for specimens of single carbon fiber/CNT/epoxy composites with different CNT treatments and bare carbon fiber. This apparent stress and apparent Young's modulus were measured in constant amplitude cyclic strain tests. The induced apparent stress for the three acid-treated CNT/epoxy composites was higher than for neat epoxy and the untreated CNT/epoxy composite samples. The apparent Young's modulus for the three acid-treated CNT was also higher than that of the untreated CNT material. These improved apparent moduli are attributed to enhanced stress transferring effects as a result of improved adhesion due to the acid treatment.

Figure 11 shows plots of induced stress and changes in electrical contact resistivity for the CNT/epoxy composites, with untreated and different CNT treatments, during five cycles of constant amplitude cyclic loading. Acetone was used as the dispersion solvent for the composites in Fig. 11. The results of these tests might be summarized as follows. The induced-stresses in the samples were significantly larger for the composites with the acid-treated CNT than for the untreated CNT, particularly for the H_2SO_4 treatment. The single carbon fiber self-sensing measurements were also distinctly different for the untreated and acid-treated CNT in composite specimens in that the changes in contact resistivity were slightly higher and exhibited more electrical noise for the acid-treated CNT composites than for the untreated case. This is attributed to differences in the electrical contact at the interface between the carbon fiber and the conductive CNT in the composites. This sensing was poorest for $Na_2Cr_2O_7 + H_2SO_4$ treated CNT composites.

3.3. Microdroplet Tests of a Carbon Fiber in Neat Epoxy and CNT/Epoxy Composites

Figure 12 shows photographs of the microdroplets for neat epoxy and CNT/epoxy composites. The fact that these microdroplets exhibited slightly different contact angles is evidence for different degrees of wetting. Figure 13 shows comparisons of the microdroplet pullout forces *versus* embedded length for the single carbon pullout tests for microdroplets of neat epoxy, as well as for untreated and sulfuric acid-treated CNT/epoxy composites. The open data markers, in Fig. 13, represent samples in which the carbon fiber pulled out while the filled-in markers are for samples where the fiber broke. This pullout force was higher for neat epoxy than it was for either the untreated or sulfuric acid-treated CNT/epoxy composites. This

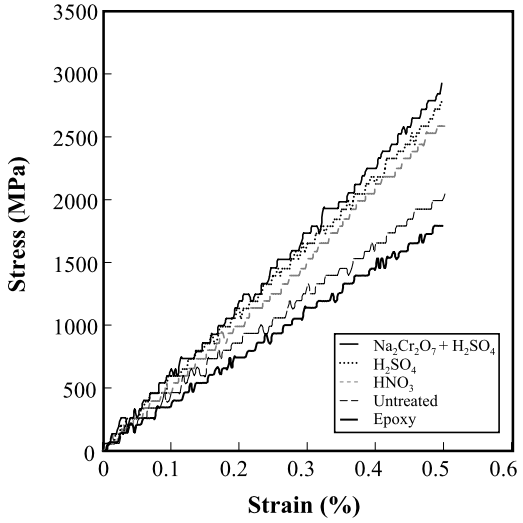

(a)

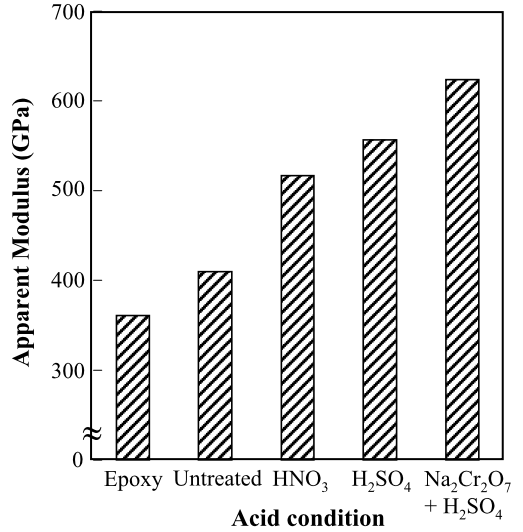

(b)

Figure 10. Apparent stress and apparent Young's modulus of 0.5 vol% single carbon fiber embedded in CNT/epoxy composites for untreated and the acid treatment conditions: (a) stress–strain and (b) apparent Young's modulus.

is attributed to significantly increased viscosity of the filled epoxy, resulting in a decrease in the interfacial shear stress (IFSS) of the CNT/epoxy composites due to poor wettability on the carbon fiber surface. Sulfuric acid-treated CNT/epoxy composites exhibited a slightly increased IFSS with the single carbon fiber surface than did the untreated CNT composite.

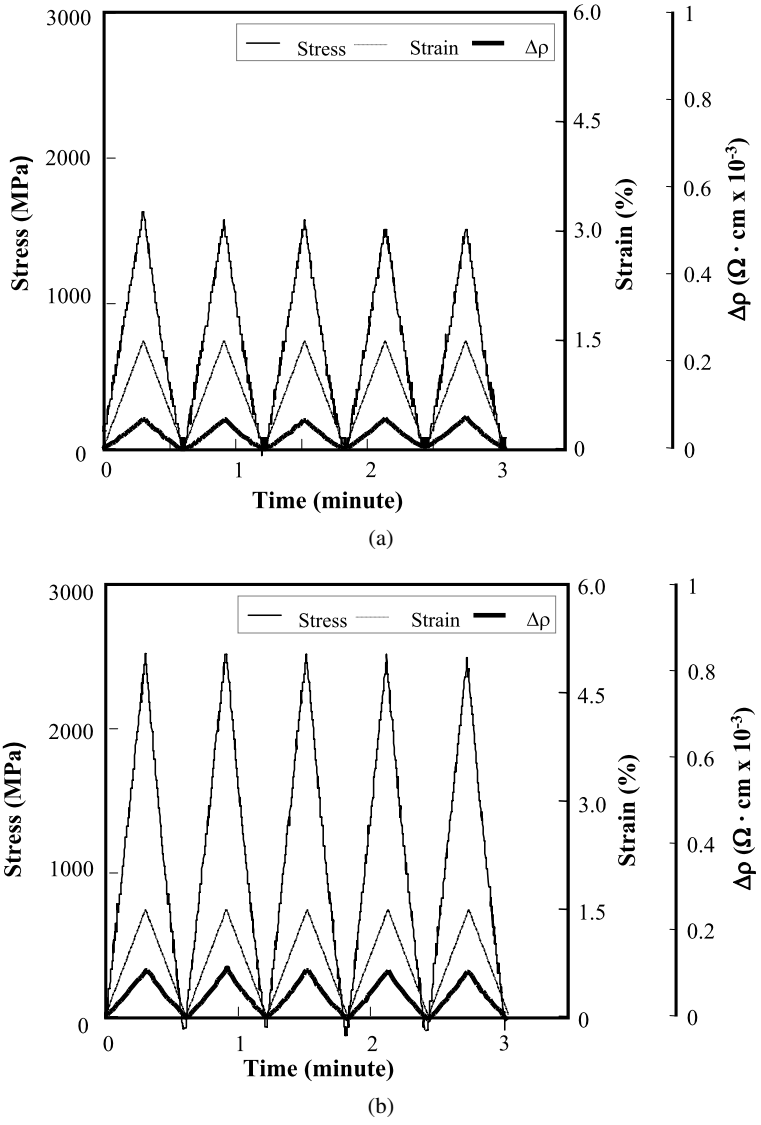

Figure 11. Induced stress and electrical contact resistivity of 0.5 vol% CNT/epoxy composites under constant amplitude cyclic strain loading: (a) untreated; (b) H_2SO_4; (c) HNO_3 and (d) $Na_2Cr_2O_7 + H_2SO_4$.

3.4. Contact Angle and Surface Energy of CNT/Epoxy Composites

Figure 14 shows static contact angle measurements for water on neat epoxy and a sulfuric acid-treated CNT/epoxy composite. This figure shows that the sulfuric acid-treated CNT/epoxy composite exhibited more hydrophobicity, whereas neat epoxy was more hydrophilic. Figure 15 shows dynamic contact forces, by the Wilhelmy plate method, in water for: (a) a single carbon fiber and (b) small

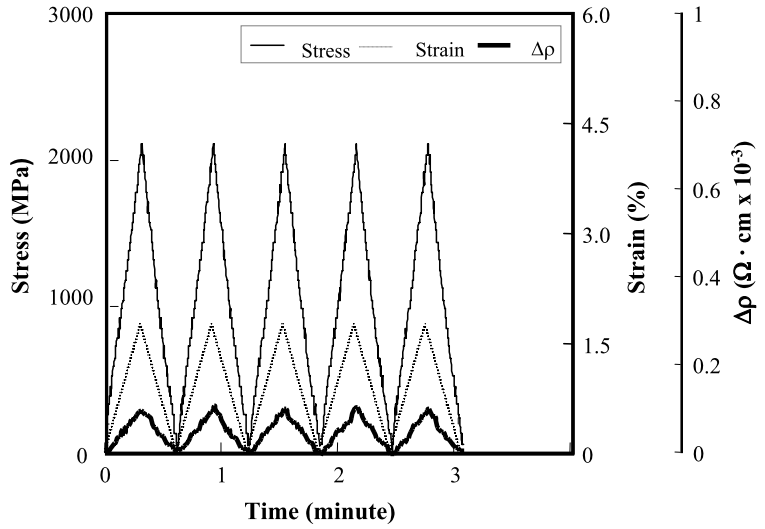

(c)

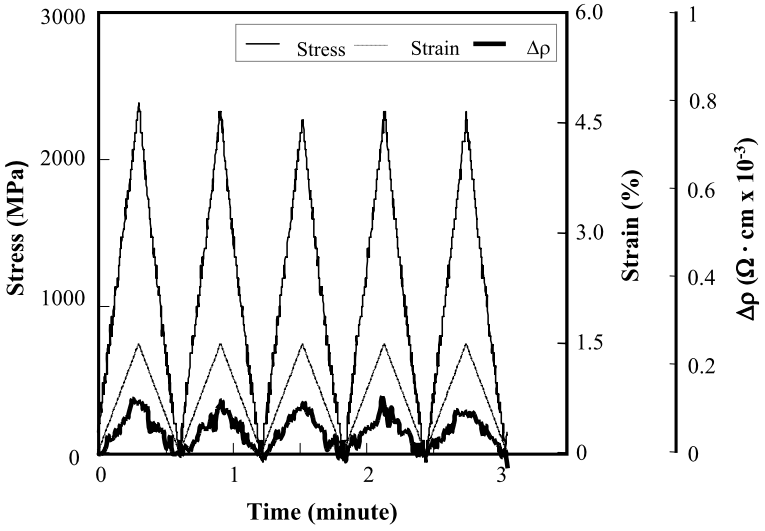

(d)

Figure 11. (Continued.)

plates of neat epoxy and various acids-treated CNT/epoxy composites. Again the CNT/epoxy composites exhibited more hydrophobicity than did neat epoxy and this hydrophobicity increased with the acid treatments. It was also noted that the contact forces of the acid-treated CNT/epoxy composites decreased with increasing dispersion. The decrease in contact force would correspond to an increase in contact angle. Therefore, the trend in the dynamic contact force measurements was entirely consistent with the observation of the static contact angles.

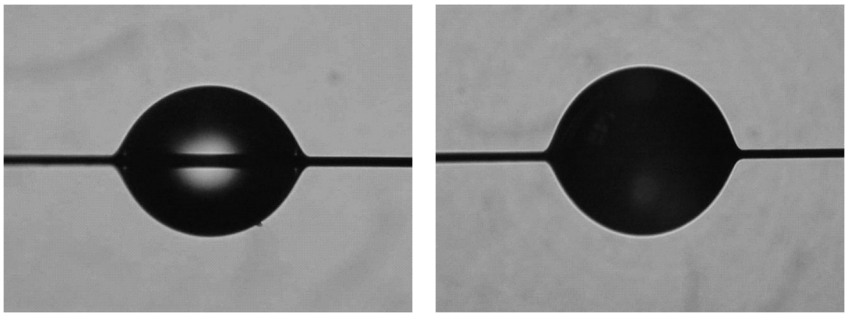

(a) (b)

Figure 12. Photograph of microdroplets on a carbon fiber: (a) neat epoxy and (b) CNT/epoxy composites.

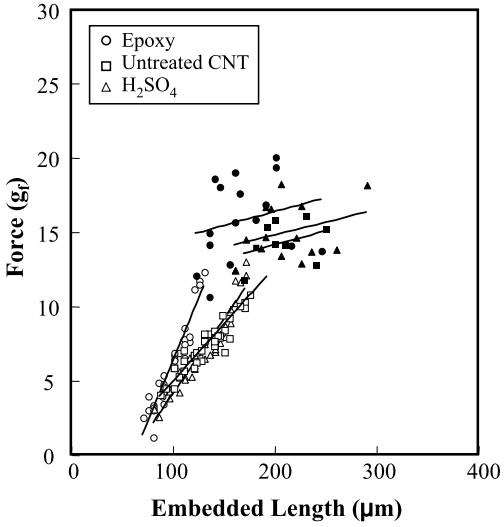

Figure 13. Comparison of carbon fiber 'pull-out' behavior for neat epoxy and CNT/epoxy composites in the microdroplet test.

Table 1 shows the acid–base surface energy components (mJ/m^2) of epoxy and CNT/epoxy composites (with untreated and three acid-treated CNT) using the four different solvents. Figure 16 shows a comparison of the work of adhesion, W_a between neat epoxy and composites of CNT with the different acid treatments. Figure 17 shows the correlation of IFSS and the apparent Young's modulus with the work of adhesion. The work of adhesion and apparent Young's modulus both increased with acid treatment of the CNT. From these two figures it is observed that the work of adhesion, W_a for sulfuric acid-treated CNT/epoxy composite was nearly the same as it was for the untreated CNT/epoxy composite, whereas the apparent Young's modulus of the sulfuric acid-treated CNT/epoxy composite was larger than it was for the untreated CNT/epoxy composite. These observations indicate that

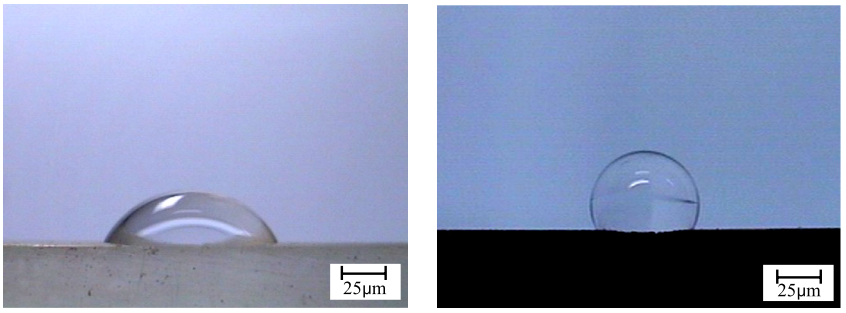

(a) (b)

Figure 14. Static contact angle for water on surfaces of: (a) neat epoxy and (b) acid-treated CNT/epoxy composites. This figure is published in color in the online version.

improved adhesion, better stress transfer IFSS, and work of adhesion all exhibited similar trends. On the other hand, the apparent Young's modulus and the work of adhesion appeared to exhibit an opposite trend.

3.5. Acoustic Emission during Sensing of Micro-damage in DMC

Figure 18 shows acoustic emission (AE), along with the stress–strain behavior, and change in electrical resistivity during the micro-damage sensing tests. The tests were conducted on DMC specimens, as previously described and shown in Fig. 4, made with sulfuric acid-treated CNT dispersed with acetone at: (a) neat epoxy; (b) 0.5 vol% untreated CNT and (c) 0.5 vol% sulfuric acid-treated CNT. Testing of the DMC specimens was at a constant rate of 0.5 mm/min in the mini-UTM. During testing, fracture of the single carbon fiber sensor occurred, often into a number of segments, as the strain progressed. For the neat epoxy specimens, the electrical resistivity increased in a sudden step to essentially infinity, at the time of the first fracture of the single carbon fiber. The specimens containing 0.5 vol% CNT (untreated and sulfuric acid-treated) exhibited very different behavior. For these DMC specimens, at the strain of first fiber fracture, a sudden (but finite) step increase in the sample's resistivity occurred. As the strain further increased, the sample's resistivity was observed to increase stepwise until, at a strain of more than double that of the first sign of fracture, the resistivity again suddenly increased to essentially infinity.

The electrical conductance of the DMC specimen involves the conductance of the single carbon fiber and conductance rendered to the composite material by the CNT filler. The resistance of the DMC specimen is a complex function, not only of the reciprocal of this electrical conductance, but it also involves the contact resistances between the carbon nanotubes and the carbon fiber fragments. The relatively small stepwise incremental resistance change patterns, shown in Fig. 18(b) and 18(c), and are attributed to successive fiber fracture during the straining. After these breaks occur, the CNT filled inner matrix provides conductive bridges across the gaps be-

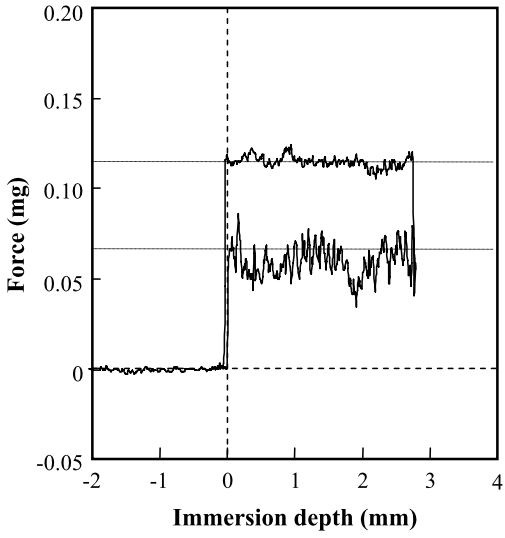

(a)

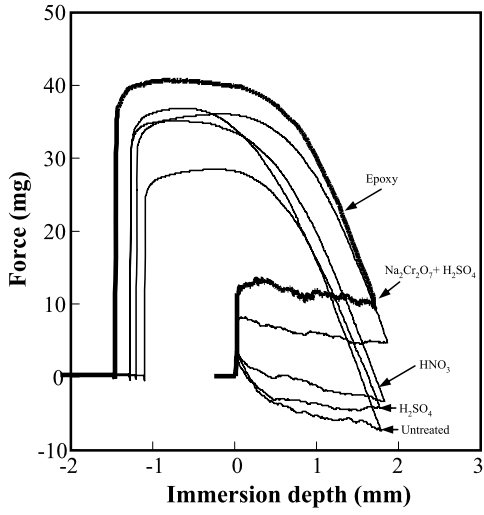

(b)

Figure 15. Wilhelmy plate forces *versus* immersion depth for dynamic contact angle for: (a) carbon fiber and (b) neat epoxy, untreated and three acid-treated CNT/epoxy composites.

tween fiber fragments. The effectiveness of these current bridges depends on the degree of dispersion.

The open and filled circles shown in the curves of Fig. 18 for the higher AE amplitudes and energies are thought to be associated with micro-carbon fiber breaks, whereas those at lower AE amplitudes and energies are probably associated with epoxy matrix cracking and/or interfacial debonding between the carbon fiber and the CNT/epoxy matrix. The neat epoxy DMC specimens failed mainly through

Table 1.
The acid–base surface energy components (mJ/m^2) of epoxy and untreated as well as three acid-treated CNT/epoxy composites using four solvents

	Condition	γ_S^{LW}	γ^-	γ^+	γ_S^T	γ^d	γ^p	W_a[1]
Epoxy	YD-114	28.2	8.1	0.0	28.7	14.7	13.6	57.6
CNT–epoxy	Untreated	24.0	1.2	0.3	24.9	21.2	2.7	54.0
	H_2SO_4	24.7	0.5	0.2	25.3	24.5	1.2	54.0
	HNO_3	31.4	0.8	0.2	32.1	29.6	1.8	60.4
	$Na_2Cr_2O_7 + H_2SO_4$	33.3	0.7	0.3	34.0	32.2	1.7	60.8

[1] Work of adhesion, W_a between a single carbon fiber and carbon nanofiber/epoxy composites.

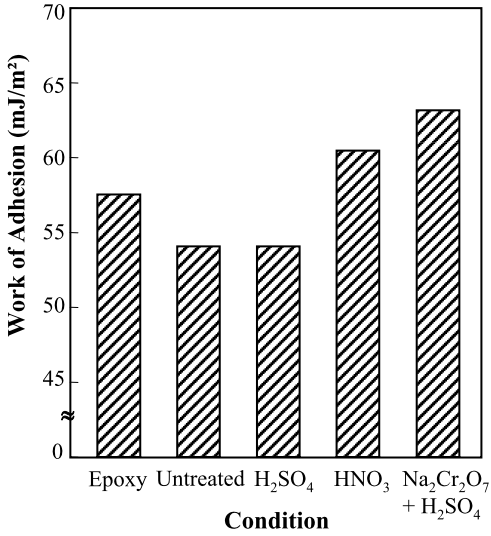

Figure 16. Comparison of the work of adhesion for neat epoxy and for composites with different CNT acid treatments.

breakage of the single carbon fibers. On the other hand, failure of the CNT/epoxy DMC specimen was much more complex involving single carbon fiber breakage, matrix cracking and debonding between the matrix at the interfaces between the epoxy and the CNT as well as the carbon fiber. For the latter case, the AE signals had significantly greater energy and somewhat greater amplitude. Another distinctive feature observed in these experiments was that the AE energy and the AE amplitude events during strain were higher for both types of CNT filled composites than they were for the specimens of neat epoxy. By strategically varying CNT acid treatment, concentration, degree of dispersion, etc. it may be possible to design composites with a trade-off between electrical and mechanical properties, thereby optimizing the composites for specific applications.

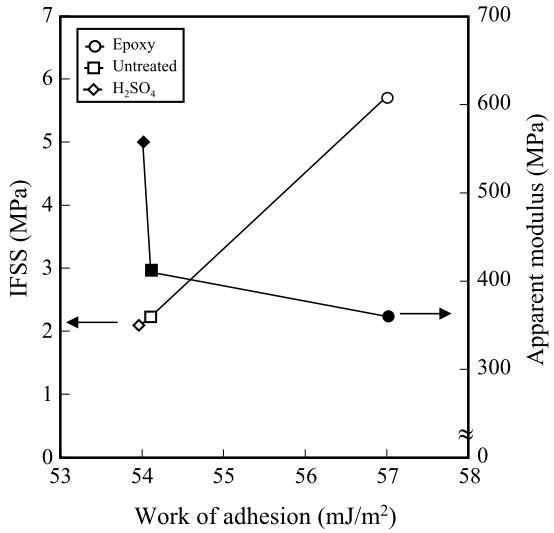

Figure 17. Apparent Young's modulus, and IFSS *versus* work of adhesion for neat epoxy and two CNT composites.

4. Conclusions

The effects of dispersing solution and acid treatment on CNT dispersion in CNT/epoxy composites was evaluated by comparing turbidity of the dispersing solution and electrical resistance, and its standard deviation. The volumetric resistivity of the composites showed a very strong dependence on the surface treatment of the CNT. The dispersing solution (water or acetone) also affects the volumetric resistivity, with acetone being the better by a factor of 4–8. The standard deviation (SD) of the volumetric resistivity was likewise strongly affected by both the acid treatment of the CNT and the dispersing solution. While the different acid treatments had some effect on dispersion, they more strongly influenced the nature of the CNT surfaces resulting in differences in amount of electrical contact, and thereby contact resistance.

The apparent Young's modulus of the sulfuric acid-treated CNT/epoxy composites was higher than that for composites with the untreated CNT. Sulfuric acid-treated CNT, with acetone was found to be the optimum conditioning for increasing the apparent Young's modulus. The electrical contact resistivity of acid-treated CNT composites exhibited more electrical noise than did untreated CNT composites. The IFSS between the single carbon fiber and CNT/epoxy was lower than it was between the single carbon fiber and neat epoxy. While the IFSS consistently increased with work of adhesion, the apparent Young's modulus decreased.

Electrical resistance measurements and acoustic emission were used to sense micro-damage during straining of the DMC specimens. The resistivity and AE portions were very distinctive. For the neat epoxy, at the time of the first fracture of the

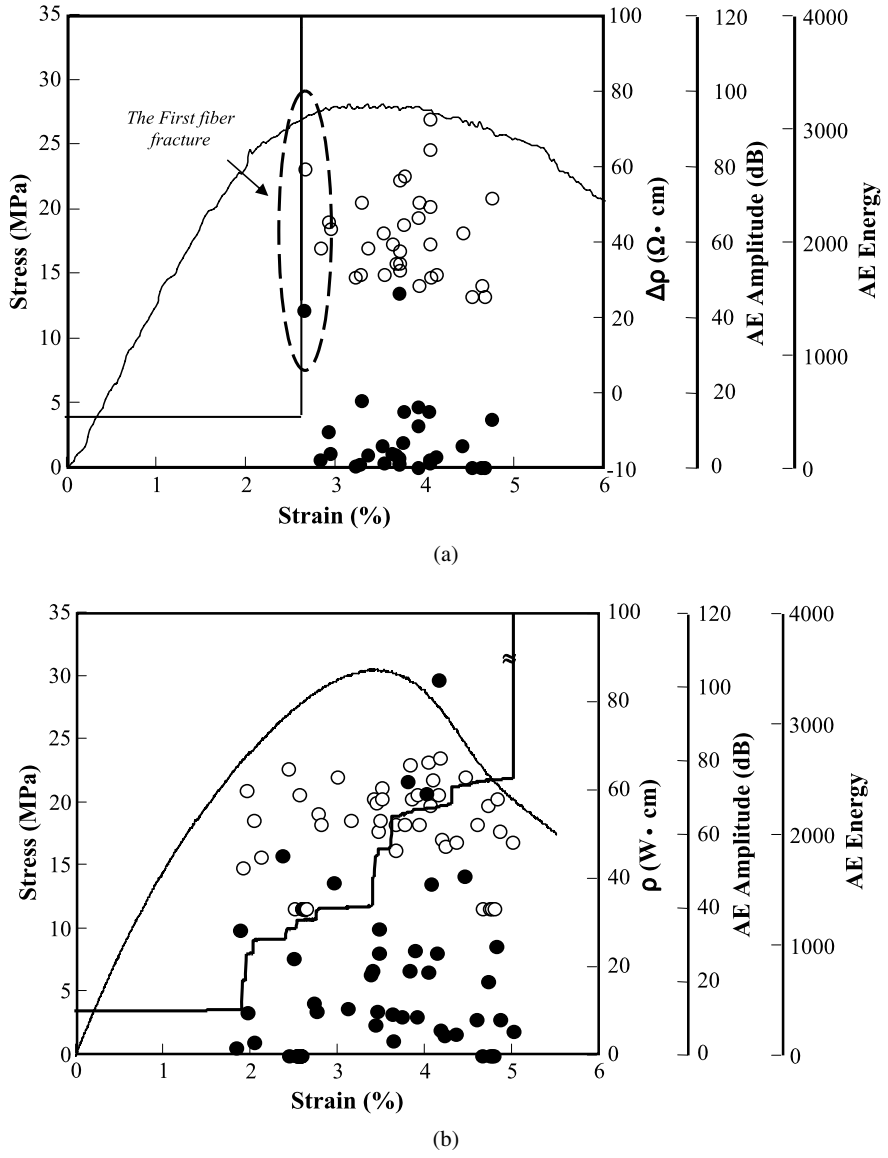

Figure 18. Plots of various measures of micro-damage *versus* strain for DMC samples with a single carbon fiber sensor for CNT/epoxy composites with: (a) neat epoxy; (b) 0.5 vol% untreated CNT and (c) 0.5 vol% H_2SO_4 CNT; open circles-AE amplitude; filled circles-AE energy.

central single carbon fiber the samples resistance increased to essentially infinity. For both types of CNT/epoxy samples the resistivity behavior was very different. At the first fiber fracture there was a sudden but finite jump in apparent resistivity as now the surrounding conductive inner composite provided an electrical bridge across the gap in the fiber.

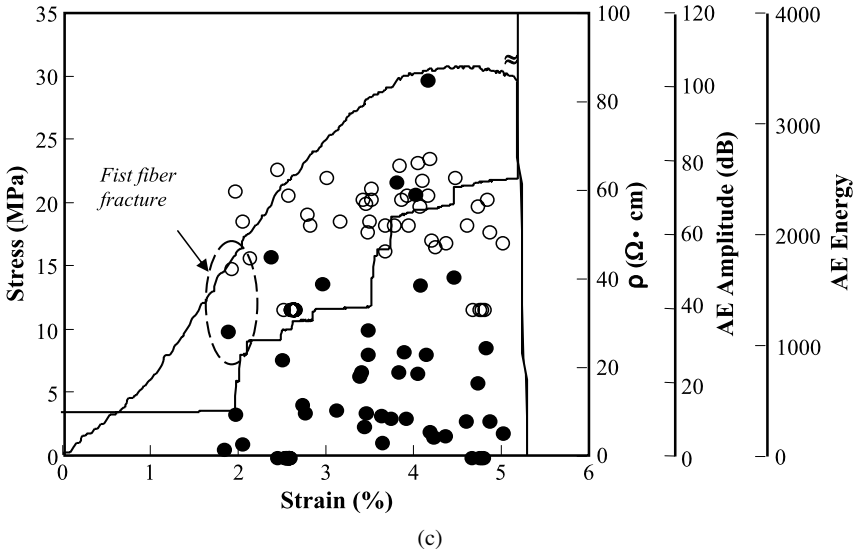

Figure 18. (Continued.)

Acknowledgements

This work was supported by the Defense Acquisition Program Administration and the Agency for Defense Development (ADD) under contract UD070009AD, 2010. Zuo-Jia Wang is grateful to the second stage of the BK21 program for its support of his fellowship.

References

1. D. Qian, E. C. Dickey, R. Andrews and T. Rantell, Load transfer and deformation mechanisms in carbon nanotube–polystyrene composites, *Appl. Phys. Lett.* **76**, 2868–2880 (2000).
2. J. Sandlera, M. S. P. Shaffera, T. Prasseb, W. Bauhoferb, K. Schultea and A. H. Windle, Development of a dispersion process for carbon nanotubes in an epoxy matrix and the resulting electrical properties, *Polymer* **40**, 5967–5971 (1991).
3. C. L. Xu, B. Q. Wei, R. Z. Ma, J. Liang, X. K. Ma and D. H. Wu, Fabrication of aluminum–carbon nanotube composites and their electrical properties, *Carbon* **37**, 855–868 (1999).
4. S. C. Chowdhury and T. Okabe, Computer simulation of carbon nanotube pull-out from polymer by the molecular dynamics method, *Composites Part A* **38**, 747–754 (2007).
5. D. D. L. Chung, Comparison of submicron-diameter carbon filaments and conventional carbon fibers as fillers in composite materials, *Carbon* **39**, 1119–1125 (2001).
6. J. Chen, A. M. Rao, S. Lyuksyutov, M. E. Itkis, M. A. Hamon, H. Hu, R. W. Cohn, P. C. Eklund, D. T. Colbert, R. E. Smalley and R. C. Haddon, Dissolution of full-length single-walled carbon nanotubes, *J. Phys. Chem. B* **105**, 2525–2528 (2001).
7. Z. Wei, C. Song and P. E. Pehrsson, Water-soluble and optically pH sensitive single-walled carbon nanotubes from surface modification, *J. Amer. Chem. Soc.* **124**, 12418–12419 (2002).

8. J. Zhu, J. D. Kim, H. Peng, J. L. Margrave, V. N. Khabashesku and E. V. Barrera, Improving the dispersion and integration of single-walled carbon nanotubes in epoxy composites through functionalization, *Nano Lett.* **3**, 1107–1113 (2003).
9. G. Zhang, S. Sun, D. Yang, J. P. Dodelet and E. Sacher, The surface analytical characterization of carbon fibers functionalized by H_2SO_4/HNO_3 treatment, *Carbon* **46**, 196–205 (2008).
10. M. A. Hamom, H. Hui, P. Bhowmik, S. Nitogi, B. Zhao, H. M. E. Itkis and R. C. Haddon, End-group and defect analysis of soluble single-walled carbon nanotubes, *Chem. Phys. Lett.* **347**, 8–12 (2001).
11. J. Liu, G. Rinzer, H. Dai, J. H. Hafner, R. K. Bradley, P. J. Boul, A. Lu, T. Iverson, K. Shelimov, C. B. Huffman, F. Rodriguez-Macias, D. T. Colbert and R. E. Smalley, Fullerene pipes, *Science* **280**, 1253–1256 (1998).
12. M. A. Hamon, H. Hui, P. Bhowmik, H. M. E. Itkis and R. C. Haddon, Ester-functionalized soluble single-walled carbon nanotubes, *Appl. Phys. A* **74**, 333–338 (2002).
13. H. Nishikiori, N. Tanaka, T. Tanigaki, M. Endo and T. Fujii, *In situ* probing of acidic groups on acid-treated carbon nanofibers using 1-aminopyrene, *J. Photochem. Photobiol. A: Chem.* **193**, 161–165 (2008).
14. P. M. Ajayan, L. S. Schadler, S. C. Giannaris and A. Rubio, Single-walled carbon nanotube–polymer composites: strength and weakness, *Adv. Mater.* **12**, 750–753 (2000).
15. J. M. Park, D. S. Kim, S. J. Kim, P. G. Kim, D. J. Yoon and K. L. DeVries, Inherent sensing and interfacial evaluation of carbon nanofiber and nanotube/epoxy composites using electrical resistance measurement and micromechanical technique, *Composites Part B* **38**, 847–861 (2007).
16. J. M. Park, S. I. Lee and K. L. DeVries, Nondestructive sensing evaluation of surface modified single-carbon fiber reinforced epoxy composites by electrical resistivity measurement, *Composites Part B* **13**, 612–626 (2006).
17. J. M. Park, D. S. Kim and S. R. Kim, Interfacial properties and microfailure degradation mechanisms of bioabsorbable fibers/poly-L-lactide composites using micromechanical and test and nondestructive acoustic emission, *Compos. Sci. Technol.* **63**, 403–419 (2003).
18. J. M. Park, D. S. Kim and S. R. Kim, Nondestructive evaluation of interfacial damage properties for plasma-treated biodegradable poly(*p*-dioxanone) fiber/poly(L-lactide) composites by micromechanical test and surface wettability, *Compos. Sci. Technol.* **64**, 847–860 (2004).
19. D. K. Owens and R. C. Wendt, Estimation of the surface free energy of polymer, *J. Appl. Polym. Sci.* **13**, 1741–1747 (1969).
20. J. M. Park, J. W. Kong, J. W. Kim and D. J. Yoon, Interfacial evaluation of electrodeposited single carbon fiber/epoxy composites by fiber fracture source location using fragmentation and acoustic emission, *Compos. Sci. Technol.* **64**, 983–999 (2004).
21. J. M. Park, P. G. Kim, J. H. Jang, Z. J. Wang, W. I. Lee, J. G. Park and K. L. DeVries, Self-sensing and dispersion evaluation of single carbon fiber/carbon nanotube (CNT)–epoxy composites using electro-micromechanical technique and nondestructive acoustic emission, *Composites Part B: Engng* **39**, 1170–1182 (2008).